Baghdad Science Journal

Volume 23 | Issue 4 Article 1

4-20-2026

Evaluating the Nuclear Structure of Some Calcium Mirror Nuclei

Sukaina Falah Hassan
Department of Physics, College of Science for Women, University of Baghdad, Baghdad, Iraq,
sakina.jabr1704@csw.uobaghdad.edu.iq

Ban Sabah Hameed
Department of Physics, College of Science for Women, University of Baghdad, Baghdad, Iraq,
bansh_phy@csw.uobaghdad.edu.iq

How to Cite this Article

Hassan, Sukaina Falah and Hameed, Ban Sabah (2026) "Evaluating the Nuclear Structure of Some Calcium Mirror Nuclei," *Baghdad Science Journal*: Vol. 23: Iss. 4, Article 1.
DOI: https://doi.org/10.21123/2411-7986.5255

BAGHDAD SCIENCE JOURNAL 2026;23(4):1116–1124

Scan the QR to view the full-text article on the journal website

RESEARCH ARTICLE

Evaluating the Nuclear Structure of Some Calcium Mirror Nuclei

Sukaina Falah Hassan, Ban Sabah Hameed *

Department of Physics, College of Science for Women, University of Baghdad, Baghdad, Iraq

ABSTRACT

In this study, we calculated the binding energy of nuclei, which holds atomic nuclei together, by utilizing electron scattering transformations in the shell model to explore the nuclear structure for proton-rich pairs of mirror nuclei: ^{34}Ca-^{34}Si, ^{0}Ca-^{35}P, ^{36}Ca-^{36}S, and ^{37}Ca-^{37}Cl. The proton envelope that surrounds the proton-rich nucleus explains why the nucleus charge and its mirror image have different radii. The wave functions for single particles were adopted from the Skyrme-Hartree-Fock approximation and Wood-Saxon potential to compute the mirror radii, mirror charge radii, and skin thickness for protons and neutrons. It was noted that the results depend on the mass numbers of the mirror nuclei and the types of wave functions. Additionally, the displacement energy of the mirror nuclei was calculated, and a mathematical relationship was found linking it with the variance in mirror charge radii. The calculated results were compared with the available practical values, where they were found to agree with the experimental data.

Keywords: Mirror nuclei, Mirror displacement energy, Proton and neutron skin, Skyrme-Hartree-Fock approximation, Wood-Saxon potential

Introduction

The Mirror Displacement Energy (MDE) and skin radii in mirror nuclei are powerful indirect tools for determining nuclear properties. The MDE has been widely used to evaluate isospin symmetry in the nuclear medium's strong interaction and to understand how nuclear structure components change concerning angular momentum. Due to isospin-breaking interactions, primarily driven by the Coulomb force, the MDE exhibits distinct energy features. This result demonstrates that by comparing the proton radii in mirror nuclei with their isotones, one can determine the neutron skin's thickness in an unstable nucleus. [1–3] The nuclear system's binding energy is influenced by the variation in nuclear asymmetry energy (E_{sy}) as the ratio of neutrons to protons fluctuates. A fundamental aspect of nuclear physics is the dual nature of nuclear systems, and energy from nuclear symmetry is essential in this context. The E_{sy} is one of the key physical quantities in the field and has a significant impact on various nuclear events and processes, where the total number of nucleons remains constant, the symmetry energy quantifies how the binding energy of the system changes as the ratio of neutrons to protons is altered. [4,5] Gaidarov et al. examined the precise measurement of the neutron skin for nuclei as a fundamental feature. They determined the difference in charge radii of a neutron-rich nucleus to determine its neutron skin and that of the corresponding mirror nuclei, this is affected by nuclear forces' charge symmetry. [6] Bano et al. conducted a study on the connection between the variations in charge radii (R_{ch}) of mirror nuclei pairs and the thickness of the neutron R_{skin}. [7] This study utilized the limited-range easy, effective interaction method and covered a wide range of masses. One of the basic features that is essential to understanding the properties of atomic nuclei is the spatial arrangement of neutrons and protons. The skin thickness of a proton or neutron, which

Received 5 April 2025; revised 17 June 2025; accepted 3 July 2025.
Available online 20 April 2026

* Corresponding author.
E-mail addresses: sakina.jabr1704@csw.uobaghdad.edu.iq (S. F. Hassan), bansh_phy@csw.uobaghdad.edu.iq (B. S. Hameed).

https://doi.org/10.21123/2411-7986.5255

is the difference in root mean square (rms) radius between the distributions of neutrons and protons, has been extensively studied by the nuclear physics community. A recent work by Novario et al.,[8] utilized first principles simulations to investigate the correlation between neutron skin thickness and isospin asymmetry in mirror nuclei. Their findings demonstrated a linear association between these quantities, consistent with the expectations of the liquid-drop model. Moreover, they measured the impact of charge symmetry breaking in the nuclear Hamiltonian, elucidating the disparities between neutron and proton radii in mirror nuclei. These findings highlight the importance of mirror nuclei research in comprehending nuclear structure and the fundamental symmetries of nuclear forces.[8] Hadron interaction has been the main method used to study neutron distribution, however, it lacks clear and accurate definitions of the interaction and reaction processes. However, theoretically sound electromagnetic methods examine the proton distribution. Interest in the variations in root-mean square radius (ΔR) has significantly increased, both in theoretical and experimental contexts.[9]

In this study, the nuclear structure of the ^{34}Ca-^{34}Si,^{35}Ca-^{35}P, ^{36}Ca-^{36}S and ^{37}Ca-^{37}Cl pairs of mirror nuclei is calculated using the Skyrme Hartree-Fock (SHF) approximation by obtaining the Skzs[10] set and Wood-Saxon potential.[11] This study will make use of the variations in the proton radii (R_{mirr}) of the mirror nuclei, the thickness of the proton and neutron skin (R_{skin}), and the mirror charges (R_{ch}^{mirr}) radii. The mirror displacement energy (MDE), for every pair was also calculated and contrasted with the available data.

Theory

The zero-range interactions known as the Skyrme forces are essentially made up of a zero-range three-body term and a momentum-dependent two-body term.[12,13]

$$V = \sum_{i<j} V_{ij}^{(2)} + \sum_{i<j<k} V_{ijk}^{(3)} \quad (1)$$

Where, $V_{ij}^{(2)}$is the two-body potential, and $V_{ijk}^{(3)}$ is the three-body potential. The total binding energy in the SHF technique is determined by adding the kinetic energy, the Coulomb energy, the pairing energy, the interaction energy between nucleons as determined by the energy density functional of Skyrme, and the correction resulting from the illusory motion.[14]

$$E = E_{Coul} + E_{kin+}E_{Sky} + E_{pair} + E_{cm} \quad (2)$$

Where, E_{Coul} is the Coulomb energy, E_{kin} is kinetic energy of the nucleons, E_{Sky} is the Skyrme energy, E_{pair} is the pairing energy, and E_c is the center-of-mass correction.

The Woods-Saxon (WS) potential is expressed in terms of a core nucleus potential given by A and Z. The energy and wave function solutions for a nucleon "in this core" will be those for both the full and empty orbitals, and it will be assumed that the relationship between these variables and experimental observables is the same as that found in the Hartree-Fock approximation. The parameters of the Woods-Saxon best fit nuclear single-particle energy and nuclear radii. The WS potential is based on a spin-independent central potential, a spin-orbit potential, and the Coulomb potential.[11]

$$V(r) = V_o(r) + V_{so}(r)\ \vec{\ell}\cdot\vec{s} + V_c(r), \quad (3)$$

Where, $V_o(r)$ is the **central potential,** $V_{so}(r)$ is the **spin-orbit potential, and** $V_c(r)$ is the Coulomb potential.

Because of the isospin symmetry of nuclear interactions, mirror nuclei with alternating proton and neutron counts should have comparable nuclear structures. If isospin symmetry is completely precise, the level schemes of mirror nuclei should be the same. Naturally, some differences arise because the isospin symmetry is broken by the Coulomb coupling. The proton or neutron skin thickness (R_{skin}) is given by:[15,16]

$$R_{skin} = R_n(Z,N) - R_p(Z,N) \quad (4)$$

where the rms radii of the neutron and proton density distributions are denoted by $R_n(Z, N)$ and $R_p(Z, N)$, respectively. Also the value of the thickness of neutron skin is equal to the value of proton skin thickness but with a negative sign. The difference between proton radii for mirror nuclei, is denoted as R_{mirr},[16] and the difference in ΔR_{ch} of root-mean-square charge radii R_{ch}, is denoted as ΔR_{ch}:[16,17]

$$R_{mirr} = R_p(Z,N) - R_p(N,Z) \quad (5)$$

$$\Delta R_{ch} = R_{ch}(Z,N) - R_{ch}(N,Z) \quad (6)$$

One important property of mirror nuclei that one wants to calculate is the nuclear mirror displacement energy. Considering the variation in the binding energies (be) of the mirror nuclei, the mirror displacement energy (MDE) is determined.[18]

$$MDE = be(Z,N) - be(N,Z) \quad (7)$$

Results and discussion

To examine the characteristics of the nuclear structure of the mirror nuclei for ^{34}Ca-^{34}Si,^{35}Ca-^{35}P,

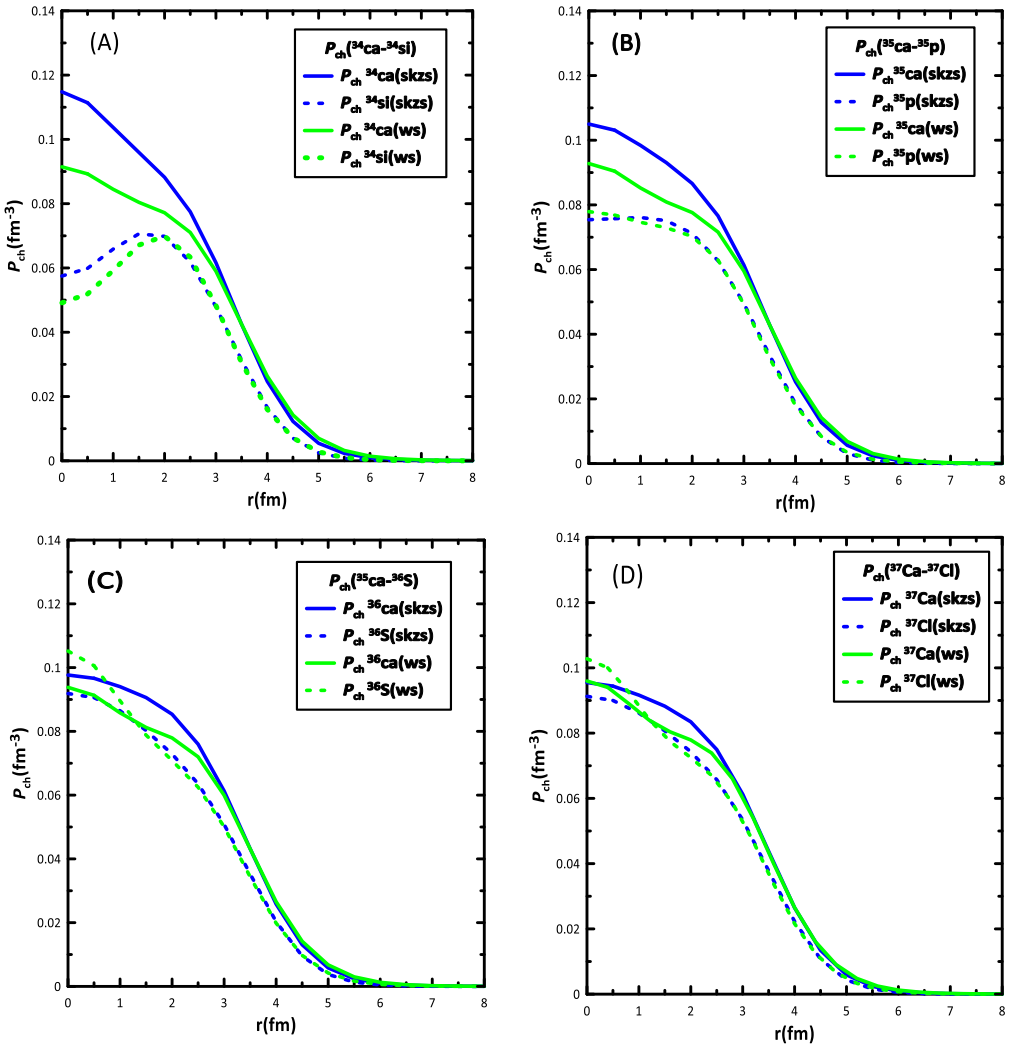

Fig. 1. (A,B,C and D). The charge density distributions $\rho_{ch}(r)$ of ^{34}Ca-^{34}Si,^{35}Ca-^{35}P, ^{36}Ca-^{36}S and ^{37}Ca-^{37}Cl pairs mirror nuclei.

^{36}Ca-^{36}S and ^{37}Ca-^{37}Cl, densities are prototyped using the SHF and WS potential.

Fig. 1 (A, B, C, and D) shows the charge density distributions ρ_{ch}(r) of the pair mirror employing the Skyrme parameters Skzs and WS potential to analyze the distinctions in the ground state properties for mirror nuclei. This figure makes it clear that the likelihood of discovering a proton close to the core section of ρ_{ch}(r) is larger than that of the tail region. In addition, the ρ_{ch}(r) values at r_0 using Skzs set are larger than values when using WS potential and at the same time, lead to closing the curves at the tail segment of ρ_{ch}(r). This explains how the addition when using Skzs parameters increases the probability that protons will shift from the nucleus's central segment to its surface, raising the nucleus's rms radius and making it less rigid than it would be when using the WS effect.

The curves in Fig. 2 (A, B, C, and D) are representative of the matter density distributions ρ_m(r) of the nuclei and their corresponding mirror, determined using Skyrme parameters and WS potentials. The data show that the calculated matter density distribution for two potentials closely corresponds with one another at r $\geq$ 2.5 fm. Also, the matter density results showed the same form, albeit in varying amounts. The range of interactions employed is the cause of this disparity, which produce distinct wave functions.

The nuclear rms radii are one of the many static properties of atomic nuclei like the protons (R_p), neutrons (R_n), matter (R_m), and charge (R_{ch}). These radii can clearly illustrate the key elements of the construction of the mirror nuclei. Since the nuclear radii are solely influenced by the diagonal matrix elements of the single particle wave function, Table 1 shows the outcome of the spatial transformation impact of protons, neutrons, and also matters with the SHF and WS wave functions after computing the nuclear radii values.

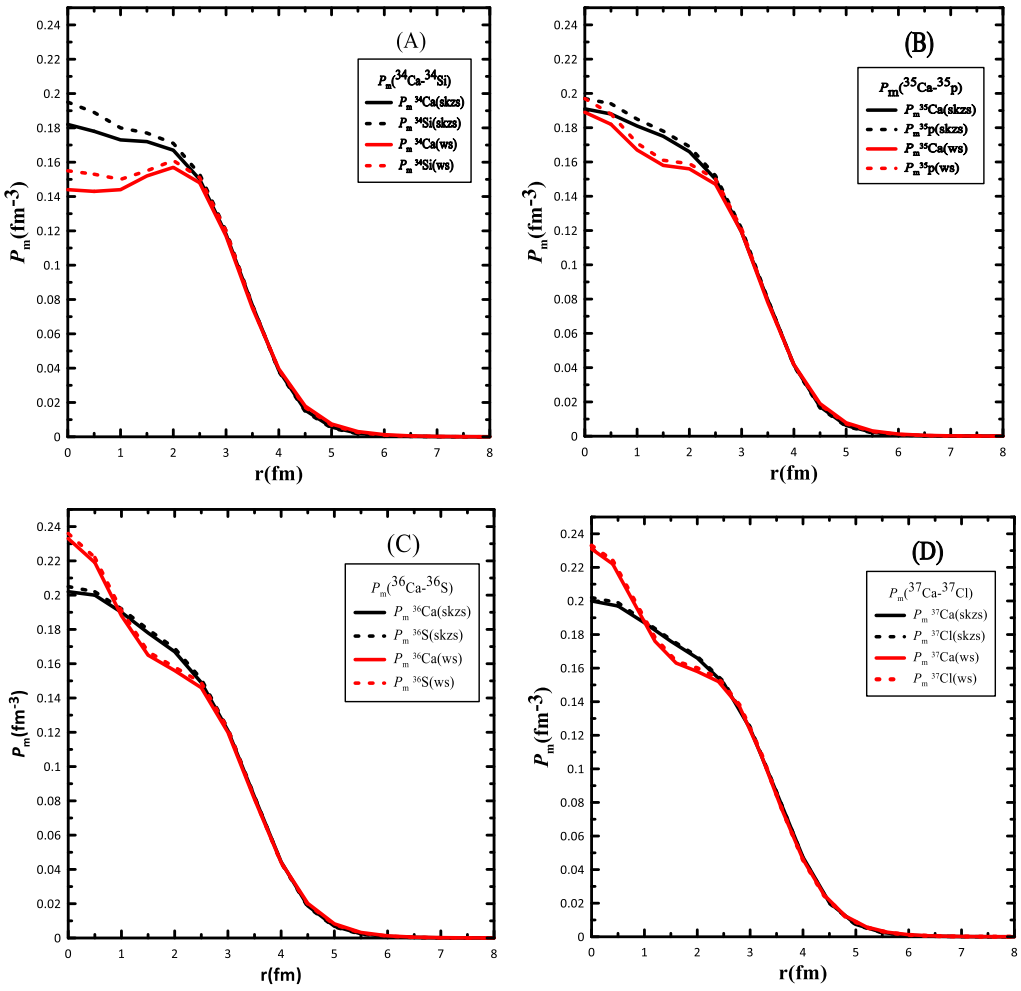

Fig. 2. (A, B, C, and D). The charge density distributions $\rho_m(r)$ of ^{34}Ca-^{34}Si,^{35}Ca-^{35}P, ^{36}Ca-^{36}S and ^{37}Ca-^{37}Cl pairs of mirror nuclei.

Table 1. The calculated rms of proton, neutron, matter and charge radii for ^{34}Ca-^{34}Si,^{35}Ca-^{35}P, ^{36}Ca-^{36}S and ^{37}Ca-^{37}Cl using SHF and WS wave functions. The calculated R_{ch} are checked with the data from experiments.[19,20].

		SHF potential				*WS potential*				
Nuclei	$J^\pi T$	R_p (fm)	R_n (fm)	R_m (fm)	R_{ch} (fm)	R_p (fm)	R_n (fm)	R_m (fm)	R_{ch} (fm)	R_{ch} (exp) (fm)
$^{34}_{20}$Ca	0^+ 3	3.310	3.069	3.213	3.387	3.487	3.073	3.323	3.561	
$^{34}_{14}$Si	0^+ 3	3.086	3.218	3.164	3.177	3.122	3.353	3.259	3.212	
$^{35}_{20}$Ca	$\frac{1}{2}^+$ $\frac{5}{2}$	3.328	3.115	3.238	3.404	3.462	3.124	3.321	3.585	
$^{35}_{15}$P	$\frac{1}{2}^+$ $\frac{5}{2}$	3.137	3.115	3.196	3.227	3.180	3.340	3.272	3.269	
$^{36}_{20}$Ca	0^+ 2	3.337	3.155	3.257	3.412	3.442	3.170	3.324	3.515	3.4493 ± 0.0044[a]
$^{36}_{16}$S	0^+ 2	3.185	3.260	3.227	3.275	3.234	3.330	3.288	3.322	3.2985 ± 0.0024[b]
$^{37}_{20}$Ca	$\frac{3}{2}^+$ $\frac{3}{2}$	3.340	3.202	3.277	3.417	3.427	3.208	3.328	3.502	3.4480 ± 0.0038[a]
$^{37}_{17}$Cl	$\frac{3}{2}^+$ $\frac{3}{2}$	3.235	3.274	3.256	3.322	3.278	3.322	3.302	3.365	3.3840 ± 0.0170[b]

a. Ref.[19], b. Ref.[20].

Fig. 3A represents the calculated value of R_{ch} with the absolute values of $|N - Z|$. The results of R_{ch} decrease except at ^{34}Ca-^{34}Si,^{35}Ca-^{35}P, where the results increase for these pairs of mirror nuclei. The calculated values for the ^{36}Ca-^{36}S and ^{37}Ca-^{37}Cl pairs of mirror nuclei are in agreement with the experimental values[19,20] when using the SHF wave function, but the results are slightly deviated from the experimental values when using the WS wave function. This indicates that there are distinct distributions of neutrons and protons within the nucleus. The values of R_m decreased linearly with the increase in the

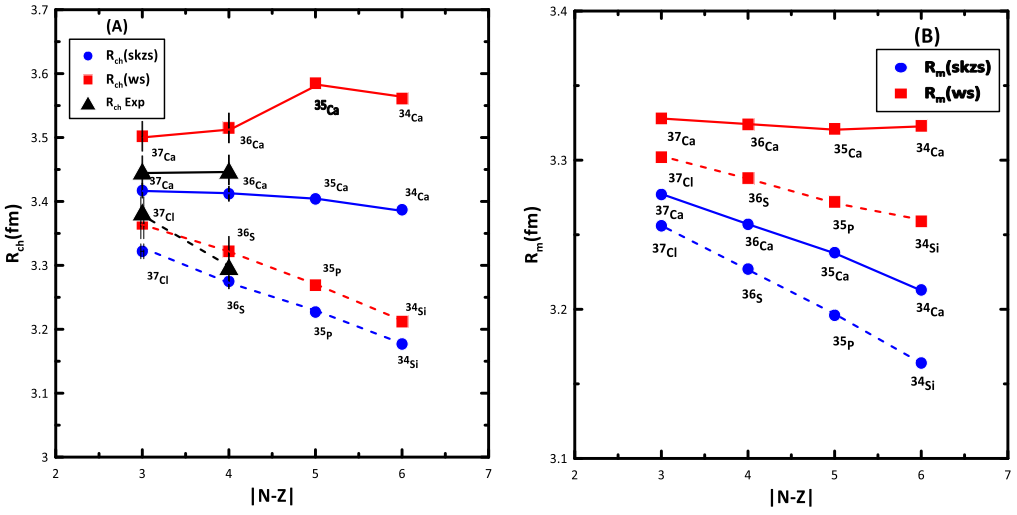

Fig. 3. (A, and B). The relationship between $|N-Z|$ the rms of charge and matter radii for ^{34}Ca-^{34}Si,^{35}Ca-^{35}P, ^{36}Ca-^{36}S and ^{37}Ca-^{37}Cl pairs of mirror nuclei using SHF and WS wave functions.

Table 2. The calculated radii of the mirror, skin, and mirror charges ^{34}Ca-^{34}Si,^{35}Ca-^{35}P, ^{36}Ca-^{36}S, and ^{37}Ca-^{37}Cl pairs of mirror nuclei using SHF and WS wave functions. The computed R_{ch}^{mirr} are comparison to the empirical data.[19,20]

	SHF potential			*WS potential*			
Mirror Nuclei	R_{mirr} (fm)	R_{ch}^{mirr} (fm)	R_{skin} (fm)	R_{mirr} (fm)	R_{ch}^{mirr} (fm)	R_{skin} (fm)	R_{ch}^{mirr} Exp. (fm)
$^{34}_{20}$Ca	0.224	0.21	–0.241	0.365	0.349	–0.414	————
$^{34}_{14}$Si			0.132			0.231	
$^{35}_{20}$Ca	0.191	0.177	–0.213	0.282	0.316	–0.338	————
$^{35}_{15}$P			0.103			0.16	
$^{36}_{20}$Ca	0.152	0.137	–0.183	0.288	0.193	–0.272	0.1508 ± 0.002
$^{36}_{16}$S			0.075			0.096	
$^{37}_{20}$Ca	0.105	0.095	–0.138	0.149	0.137	–0.219	0.064 ± 0.0132
$^{37}_{17}$Cl			0.039			0.044	

absolute values of $|N-Z|$ for all mirror nuclei. This relation is shown in Fig. 3B. Also, from the figure, one can conclude that the WS wave function is dominant.

Table 2 shows the results of the R_{skin}, R_{mirr} and R_{ch}^{mirr} are calculated using two different potentials, WS and SHF, to observe the impact of the calculation method on the results. There is a noticeable variation in the values computed between the two models for different nuclei. Also, significant differences are observed between different nuclei; these differences reflect changes in the distribution of mass and neutrons within the nucleus. The R_{mirr} and R_{ch}^{mirr} radii decrease when moving from one isotope to another, which is consistent with changes in the number of neutrons and protons in the nucleus.

The information in Fig. 4 demonstrates that the nuclear model employed affects the ΔR_{skin}calculation for mirror nuclei, and these values vary according to the nucleus's atomic and neutron numbers.

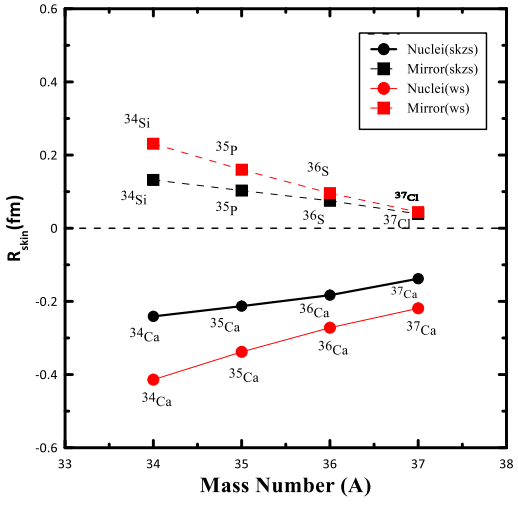

Fig. 4. The relationship between the mass number and ΔR_{skin} of the ^{34}Ca-^{34}Si,^{35}Ca-^{35}P, ^{36}Ca-^{36}S and ^{37}Ca-^{37}Cl pairs mirror nuclei using SHF and WS wave functions.

Understanding nuclear interactions and the characteristics of various chemical elements requires an understanding of how the nuclear structure changes for nuclei with varied proton and neutron counts, which is reflected in these computations. Understanding how small nuclei interact with one another and how these interactions impact the stability of nuclear aggregation is what makes studying MDE in the setting of nuclear clusters so important. It may also find use in several domains, including nuclear physics, nuclear astrophysics, and nuclear energy development. Since the WS model employs a symmetrical distribution of nuclear mass (*i.e.*, density distribution) in the form of a smooth and symmetrical surface, the MDE of the mirror nucleus is zero. Over time, the transition from high density inside the nucleus to low density outside the nucleus occurs gradually. Because of its distribution, the nucleus is regarded as symmetrical and uniform.

In the SHF model, even if the nucleus is symmetric, interactions between the nuclear density and the internal field resulting from this density can lead to slight distortions in the shape of the nucleus. As a result, the displacement energy cannot be exactly zero, as it depends on the distribution and internal interactions between the components of the nucleus. Therefore, the SHF approximation was used to investigate the MDE of the mirror nucleus. The SHF model integrates density-dependent interactions and a more detailed analysis of nucleon correlations, which may account for its superior alignment with experimental neutron skin measurements in neutron-rich mirror nuclei. Simultaneously, the WS model, due to its phenomenological nature, may exhibit insensitivity to nuanced isospin-breaking effects, especially those stemming from the spatial extension of the neutron distribution and Coulomb repulsion un proton-rich systems.

Table 3. The computed values of the MDE for ^{34}Ca-^{34}Si,^{35}Ca-^{35}P, ^{36}Ca-^{36}S, and ^{37}Ca-^{37}Cl pairs of mirror nuclei using SHF potential. The results are checked with the data from experiments of Ref.[21].

Mirror Nuclei	MDE(Mev)	
Skzs set	Cal.	Exp.[21]
$^{34}_{20}$Ca $^{34}_{14}$Si	37.9368	37.852
$^{35}_{20}$Ca $^{35}_{15}$P	32.2982	33.37
$^{36}_{20}$Ca $^{36}_{16}$S	26.2649	27.354
$^{37}_{20}$Ca $^{37}_{17}$Cl	20.146	20.948

Table 3 shows the comparison between the calculated values and experimental data for MDE. The calculated results are very consistent with practical values.[21]

Fig. 5 shows the relationship between the mass numbers (A) and the MDE. From the figure one can notice that the values of MDE decrease linearly with the increase in the mass number of the mirror nuclei. This is due to the effects of nuclear interactions and quantum effects that contribute to changing the internal distribution of protons and neutrons. Fig. 6 shows the relationship between the R_{ch}^{mirr} and the MDE. In general, when the nuclear mirror charge radius

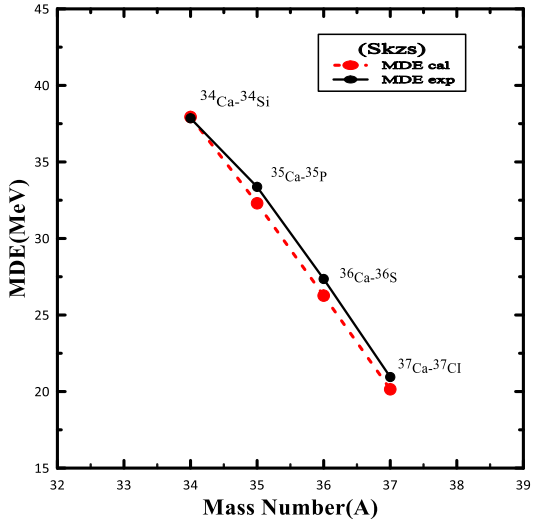

Fig. 5. The relationship between the mass number and MDE for the ^{34}Ca-^{34}Si,^{35}Ca-^{35}P, ^{36}Ca-^{36}S, and ^{37}Ca-^{37}Cl pairs of mirror nuclei. The experimental data from Ref.[21].

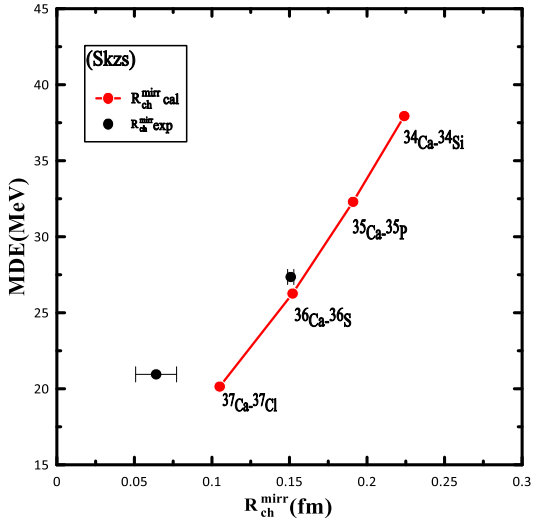

Fig. 6. The relationship between the R_{mirr}^{ch} and MDE for the ^{34}Ca-^{34}Si,^{35}Ca-^{35}P, ^{36}Ca-^{36}S, and ^{37}Ca-^{37}Cl pairs of mirror nuclei. The experimental data from Ref.[21].

increases, the MDE decreases. This makes sense since a higher charge radius disperses the charge distribution over a greater volume, lowering the protons' and neutrons' mutual interactions. In contrast to smaller nuclei, where interactions are greater, larger nuclei need less energy to extract a proton or neutron.

Conclusion

This study used the Skyrme-Hartree-Fock approximation and Wood-Saxon potentials to analyze the nuclear structure for pairs of mirror nuclei with varying masses (34, 35, 36, and 37). For the pair of mirrors using two potentials, the matter density distributions ρ_m(r) diverge at r less than 2.5 fm and firmly align at r $>$ 2.5 fm. This disparity arises from the range of potentials used, which results in different wave functions. Also, while using the Skzs set, the ρ_{ch}(r) values at r_0 are bigger than when using the WS potential, which causes the curves in the tail segment of ρ_{ch}(r) to close.

The value of R_m exhibited a decrease when the $|N-Z|$ it is increased for all mirror nuclei. But the values of R_{ch} decrease at the mass numbers 36 and 37, while R_{ch} increases at the mass numbers 34 and 35. These numbers line up with the observations. The difference in the kinetic energy operator used for protons and neutrons, which have different masses, is the cause of this phenomenon. The results of the R_{skin}, R_{mirr} and R_{ch}^{mirr} depend on the mass numbers of mirror nuclei and the kinds of potentials. The MDE was calculated, and there is very good agreement with practical values of the mirror nuclei. We also found that the relationship between MDE and R_{ch}^{mirr} is an inverse relationship.

Acknowledgements

This study is for research purposes only, and it is clarified that no external funding was received. Also, we would like to extend our appreciation to department of physics, College of Science for Women, University of Baghdad, for their collaboration in facilitating this research.

Authors' declaration

- Conflicts of Interest: None.
- We hereby confirm that all the Figures and Tables in the manuscript are ours. Furthermore, any Figures and images that are not ours have been included with the necessary permission for republication, which is attached to the manuscript.
- No animal studies are present in the manuscript.
- No human studies are present in the manuscript.
- Ethical Clearance: The project was approved by the local ethical committee at University of Baghdad.

Authors' contribution statement

S.F.H. and B.S.H. both contributed to visualizing and designing the study, obtaining data, in addition to analyzing and interpreting the results, and writing the manuscript.

Data availability

The datasets generated and analyzed during the current study are available in the Tables 1 to 3 and Figs. 3, 5 and 6 repository at https://doi.org/10.1016/j.adt.2021.101440, https://doi.org/10.1016/j.adt.2011.12.006 and https://doi.org/10.1088/1674-1137/abddaf.

References

1. Yang J and Piekarewicz J. Difference in proton radii of mirror nuclei as a possible surrogate for the neutron skin. Phys. Rev. C. 2018 Jan;97:014314. https://doi.org/10.1103/PhysRevC.97.014314.
2. Boso A, Lenzi S M, Recchia F, Bonaard J, Zuker A P, Aydin S, Bentley, *et al.* Neutron skin effects in mirror energy differences: The case of ^{23}Mg- ^{23}Na. Phys Rev Lett. 2018 July;121:032502. https://doi.org/10.1103/PhysRevLett.121.032502.
3. Hamza S S and Hameed B S. Study of the relationship for neutron and proton skin thickness on the neutron equation of state for ^{18}Ne-^{18}O pair mirror nuclei. Baghdad Sci J. 2025 Jan.;22(1):198–207. https://doi.org/10.21123/bsj.2024.10512.
4. Jiang W, Forssén C, Djärv T and Hagen G. Nuclear-matter saturation and symmetry energy within Δ-full chiral effective field theory. Phys. Rev. C. 2024 June;109:L061302. https://doi.org/10.1103/PhysRevC.109.L061302.
5. Ravlic A, Yuksel E, Niksic T. and Paar N. Influence of the symmetry energy on the nuclear binding energies and the neutron drip line position Phys. Rev. C. 2023 Nov.;108:054305. https://doi.org/10.1103/PhysRevC.108.054305.
6. Gaidarov M, Moumene I, Antonov A, Kadrev D, Sarriguren P. and de Guerra E. Proton and neutron skins and symmetry energy of mirror nuclei. Nucl Phys A. 2020 Dec.;1004:122061. https://doi.org/10.1016/j.nuclphysa.2020.122061.
7. Bano P, Pattnaik S, Centelles M, Viñas X and Routray T. Correlations between charge radii differences of mirror nuclei and stellar observables. Phys. Rev. C. 2023 July;108:015802. https://doi.org/10.1103/PhysRevC.108.015802.
8. Novario S. J., Lonardoni D., Gandolfi S. and Hagen G. Trends of neutron skins and radii of mirror nuclei from first principles. Phys. Rev. Lett. 2023 Jan.;130:032501. https://dx.doi.org/10.1103/PhysRevLett.130.032501.

9. Suzuki T. The relationship of the neutron skin thickness to the symmetry energy and its slope. Prog. Theor. Exp. Phys. 2022 June;2022:063D01. https://doi.org/10.1093/ptep/ptac083.
10. Brown B and Rae W. The shell-model code NuShellX@ MSU. Nucl Data Sheets. 2014 June;120:115–118. https://doi.org/10.1016/j.nds.2014.07.022.
11. Gonul B and Koksal K. A note on the woods-saxon potential. Phys. Scr. 2007 Oct.;76:565–570. https://doi.org/10.1088/0031-8949/76/5/026.
12. Rafid A. H. Asal and Wissam A. Ameen, Charge shift in He isoelectronic series using the Hartree-Fock method, AIP Conf. Proc. 2025 April;3282:020016. https://doi.org/10.1063/5.0264841.
13. Radhi R, Alzubadi A and Manie S., Electromagnetic multipoles of positive parity states in ^{27}Al by elastic and inelastic electron scattering. Nucl Phys A. 2021 Nov.;1015:122302. https://doi.org/10.1016/j.nuclphysa.2021.122302.
14. Hamza S S and Hameed B S. Study of the nuclear structure for ^{19}Ne-^{19}F and ^{21}Ne-^{21}Na mirror nuclei using nuclear equation of state. AIP Conf. Proc. 2025 April;3282:020006. https://doi.org/10.1063/5.0265950.
15. Xayavong L and Lim Y. Shell-model description of the isospin-symmetry-breaking correction to gamow-teller β-decay rates and their mirror asymmetries. arXiv:2312.07900 [nucl-th]. 2023 Dec.:1–21. https://doi.org/10.48550/arXiv.2312.07900.
16. Yao Xua J, Zheng Li Z, Hua Suna B, Fei Niu Y, Roca- Mazac X, Sagawad H and Tanihata I. Constraining equation of state of nuclear matter by charge-changing cross section measurements of mirror nuclei. Phys Lett B. 2022 Oct.;833:137333. https://doi.org/10.1016/j.physletb.2022.137333.
17. Kumar P, Bishakha N, Thakur V, Kumar R and Dhiman S. A study of trends of neutron skin thickness and proton radii of mirror nuclei. In Proceedings of the DAE Symp. Nucl Phys. 2022 Dec.;2:300–301. https://doi.org/10.1142/S0217732324500226.
18. Bentley M. Excited states in isobaric multiplets-experimental advances and the shell-model approach. Phys. 2022 Sep.;4(3):995–1011. https://doi.org/10.3390/physics4030066.
19. Li T, Luo Y and Wang N. Compilation of recent nuclear ground state charge radius measurements and tests for models. At. Data Nucl. Data Tabl. 2021 July;140:101440. https://doi.org/10.1016/j.adt.2021.101440.
20. Angeli I and Marinova K. Table of experimental nuclear ground state charge radii: An update. At Data Nucl. Data Tabl. 2013;99(1):69–95. https://doi.org/10.1016/j.adt.2011.12.006.
21. Wang C M, Huang W, Kondev F, Audi G and Naimi S. The Ame2020 atomic mass evaluation (II). Tables, graphs and references. Chin Phys C. 2021 March;45(3):030003. https://doi.org/10.1088/1674-1137/abddaf.

تقييم البنية النووية لبعض نوى الكالسيوم المرآتية

سكينة فلاح حسن، بان صباح حميد

قسم الفيزياء، كلية العلوم للبنات، جامعة بغداد، بغداد، العراق.

الخلاصة

في هذه الدراسة، تم حساب طاقة الرابط النووي، التي تربط النوى الذرية ببعضها، بأستخدم تحويلات تشتت الإلكترونات في نموذج الغلاف لاستكشاف البنية النووية لأزواج النوى المرآتية الغنية بالبروتونات: ^{36}Ca-^{36}S، ^{35}Ca-^{35}P، ^{34}Ca-^{34}Si، و^{37}Ca-^{37}Cl. يُفسر سمك القشرة البروتون المحيط بالنواة الغنية بالبروتونات سبب اختلاف نصف قطر شحنة النواة وصورتها المرآتية. استُخدمت الدوال الموجية للجسيمات المفردة من تقريب سكايرم-هارتري-فوك وجهد وود- ساكسون لحساب نصف قطر المرآة، ونصف قطر شحنتها، وسمك القشرة الخارجي للبروتونات والنيوترونات. لوحظ أن النتائج تعتمد على الأعداد الكتلية للنوى المرآتية وأنواع الدوال الموجية. بالإضافة إلى ذلك، حُسبت طاقة إزاحة النوى المرآتية، ووُجدت علاقة رياضية تربطها بالتباين في نصف قطر شحنة المرآة. وتمت مقارنة النتائج المحسوبة مع القيم العملية المتوفرة حيث وجد أنها تتفق مع البيانات التجريبية.

الكلمات المفتاحية: النوى المرآتية، طاقة الإزاحة المرآتية، سمك القشرة للبروتون والنيوترون، تقريب سكيرم-هارتري-فوك، جهد وود – ساكسون.